



PCCP

Simple analysis of crystal growth in a finite space

Journal:	<i>Physical Chemistry Chemical Physics</i>
Manuscript ID	CP-ART-01-2022-000260.R1
Article Type:	Paper
Date Submitted by the Author:	22-Mar-2022
Complete List of Authors:	Yang, Fuqian; University of Kentucky, Chemical and Materials Engineering

SCHOLARONE™
Manuscripts

Modeling analysis of the growth of a cubic crystal in a finite space

Fuqian Yang

Materials Program, Department of Chemical and Materials Engineering

University of Kentucky, Lexington KY 40506, USA

fuqian.yang@uky.edu

Abstract

The applications of semiconductor nanocrystals in optoelectronics are based on the unique characteristic of quantum confinement. There is great interest to tailor the performance of optoelectronic nanodevices and systems through the control of the sizes of nanocrystals. In this work, we develop a general mathematical formulation for the growth of a crystal/particle in a liquid solution, which takes account of the combinational effect of diffusion-limited growth and reaction-limited growth, and formulate the growth equations for the size of a cubic crystal grown under three different scenarios - isothermal and isochoric condition, isothermal growth with evaporation and/or extraction of solvent and isochoric growth with the change in temperature. For the growth of a cubic crystal under isothermal and isochoric conditions, there are three growth stages – linear growth, nonlinear growth and plateau, and the growth rate in the stage of linear growth and the final size of the cubic crystal are dependent on the degree of supersaturation. For the growth of multi-crystals with a Gaussian distribution of crystal sizes, the change of the monomer concentration in a liquid solution is dependent on the change rates of average size and the standard deviation of the crystal sizes.

Keywords: Crystal growth; Diffusion-limited growth; Reaction-limited growth; Finite space.

Introduction

Inorganic and hybrid halide perovskites have exhibited great potential for the applications in optoelectronics and energy conversion due to the unique properties, including size-dependent bandgap, large optical absorption and facile synthesis processes¹⁻¹¹. For example, a power conversion efficiency of ~29% for perovskite-based solar cells, which is better than the efficiency of polysilicon-based solar cells, was recently reported by Al-Ashouri et al.¹², and an external quantum efficiency of more than 20%, which is comparable to commercial organic LEDs, was also reported^{4, 5, 13}.

The performance of perovskite-based optoelectronic devices and solar cells is dependent on the quality of perovskite crystals, and the optoelectronic devices and solar cells made from perovskite single crystals exhibit much better performance than those made from perovskite polycrystals. There is a great need to produce perovskite single crystals of large sizes. Currently, there are few solution-based techniques available to produce halide perovskites of large sizes, including inverse-temperature method^{14, 15}, temperature-cooling method¹⁶, antisolvent evaporation¹⁷ and extraction of solvent¹⁸. In the heart of these techniques is either the increase of the monomer concentration or the decrease of the solubility to increase the degree of supersaturation. Note that the inverse-temperature method is based on the the decrease of the solubility with increasing temperature, i.e., increasing temperature can immediately make the liquid solution supersaturated and the antisolvent method is based on the immediate formation of nuclei when the precursor solution is mixed with antisolvent, as reported by Zhang et al.¹⁹ and used extensively in the synthesis of halide perovskite nanocrystals.

There are two processes likely controlling the growth of crystals in a solution – one is diffusion, and the other is surface reaction²⁰⁻²³. Currently, most studies have been based on an infinite system without considering the change in the solubility and the effect of crystal size²⁰⁻²². Recently, Yang²³ analysed the growth of a spherical crystal controlled by diffusion in a finite space without the contribution of surface reaction. The numerical results revealed that there are two growth stages – the crystal size is a linearly increasing function of the growth time in the first growth stage and a power function of the growth time in the second growth stage. Following the method given by Sung et al.²⁰ in the discussion of the effect of crystal size/mass on the growth behavior, Liu et al.²⁴ obtained a relationship between the time derivative of the crystal

mass and the ramp rate of temperature, and Yao et al.¹⁸ obtained a relationship between the time derivative of the crystal mass and the change rate of the liquid solution. However, both relationships are questionable, and the authors did not provide any explicit formulation for the temporal evolution of the monomer concentration during the crystal growth.

Realizing the important applications of halide perovskites in optoelectronics and the need to grow halide perovskites of large sizes, we follow the approach given by Sung et al.²⁰ to analyze the growth of a single crystal in a solution without solving the diffusion problem. In contrast to the work by Sung et al.²⁰, we develop a general formulation, which takes into account the effects of the loss of solvent and the change of solubility.

Mathematic Formulation

Considering the growth of a crystal in a liquid solution, as shown in Fig. 1. At the outset of growth ($t = 0$) at temperature T_0 , the concentration of monomers (solute atoms/molecules) is C_0 in the unit of mole per unit volume, the volume of the space consisting of the liquid solution and the crystal is V_0 , and the mass of the crystal is M_0 . At time t and temperature T , the concentration of monomers is C in the unit of mole per unit volume, the volume of the space consisting of the liquid solution and the crystal is V , and the mass of the crystal is M .



Figure 1. Growth of a cubic crystal of a in width in a liquid solution. The thickness of diffusion layer is δ .

The mass conservation gives

$$C_0 \left(V_0 - \frac{M_0}{\rho} \right) = \int_{\bar{V}} C dV + \frac{M - M_0}{\rho \Omega} \quad (1)$$

where ρ and Ω are the density and molar volume of the crystal, respectively, M_0/ρ is the volume of the crystal at the outset of growth, \bar{V} represents the space occupied by the liquid solution. In general, one needs to have the spatial distribution of the monomer concentration in the calculation of the integral in Eq. (1).

For simplification, we use the assumption by Sung et al.²⁰ in the study of the growth of yttrium oxalate in a supersaturated solution that the monomer concentration is uniformly distributed and is only dependent on time and temperature. Therefore, Eq. (1) is simplified to as

$$C_0 \left(V_0 - \frac{M_0}{\rho} \right) = C \left(V - \frac{M}{\rho} \right) + \frac{M - M_0}{\rho \Omega} \quad (2)$$

Taking derivative of Eq. (2) with respect to the growth time, we obtain

$$\left(V - \frac{M}{\rho} \right) \frac{dC}{dt} + C \frac{dV}{dt} + \frac{1 - \Omega C}{\rho \Omega} \frac{dM}{dt} = 0 \quad (3)$$

It is evident that the growth of the crystal is dependent on the temporal evolution of the monomer concentration and the volume of the system.

As discussed above, there are two processes controlling the growth of the crystal – one is diffusion, and the other is surface reaction. For the monomer diffusion in the liquid solution, we have the molar flux of monomers in the liquid solution onto the crystal as

$$\mathbf{j} \cdot \mathbf{n} \Big|_{\text{surface}} = -D \frac{C - C_i}{\delta} \quad (4)$$

where \mathbf{j} is the molar flux of the monomers in the liquid solution, \mathbf{n} is the outward unit normal of the crystal surface, D is the diffusivity of the monomers in the liquid solution, C_i is the monomer concentration on the surface of the crystal, and δ is the thickness of the diffusion layer near the crystal surface. Assuming the first-order surface reaction and using the mass conservation for the monomers, we have

$$\mathbf{j} \cdot \mathbf{n} \Big|_{\text{surface}} = -k(C_i - C_s) \quad (5)$$

with k as the reaction rate for the surface reaction and C_s as the solubility of the crystal at temperature T . Note that Sung et al.²⁰ assumed a power-law dependence of the surface reaction on the concentration difference ($C_i - C_s$). Such a situation can occur only for a significant difference between C_i and C_s and/or under external influence. Here, we are focused only on the first-order surface reaction.

Substituting Eq. (5) in Eq. (4) yields

$$C_i = \frac{DC + k\delta C_s}{D + k\delta} \quad (6)$$

which gives

$$\mathbf{j} \cdot \mathbf{n}|_{\text{surface}} = -\frac{kD(C - C_s)}{D + k\delta} \quad (7)$$

Thus, the increase rate of the crystal volume can be calculated as

$$\frac{dV_c}{dt} = \Omega \int_S (-\mathbf{j} \cdot \mathbf{n}|_{\text{surface}}) dS = \frac{kD\Omega(C - C_s)S}{D + k\delta} \quad (8)$$

with V_c and S as the crystal volume and the surface area of the crystal at the growth time t . From Eq. (8), we obtain the increase rate of the crystal mass and the monomer concentration as

$$\frac{dM}{dt} = \rho \frac{dV_c}{dt} = \frac{kD\rho\Omega(C - C_s)S}{D + k\delta} \quad \text{and} \quad C = \frac{D + k\delta}{kD\rho\Omega} \frac{1}{S} \frac{dM}{dt} + C_s \quad (9)$$

Substituting the second equation in Eq. (9) in Eq. (3), we obtain the differential equation for the growth rate of the crystal mass as

$$\left(V - \frac{M}{\rho} \right) \left[\frac{D + k\delta}{kD\rho\Omega} \frac{d}{dt} \left(\frac{1}{S} \frac{dM}{dt} \right) + \frac{dC_s}{dt} \right] + \left(\frac{D + k\delta}{kD\rho\Omega} \frac{1}{S} \frac{dM}{dt} + C_s \right) \frac{dV}{dt} + \frac{1}{\rho\Omega} \left[1 - \frac{D + k\delta}{kD\rho} \frac{1}{S} \frac{dM}{dt} - \Omega C_s \right] \frac{dM}{dt} = 0 \quad (10)$$

Assuming that the geometrical shape of the crystal during the growth remains unchanged, i.e. there is a similarity of the geometry of the crystal at any two different growth times. Such an assumption has been implicitly used in most studies of crystal growth. Thus, the change of M is proportional to the surface area of the crystal with the proportionality being the density and the change in the characteristic dimension of the crystal. Therefore, Eq. (10) provides the base to analyze the temporal evolution of the crystal, which takes into account the change in the solubility and the system volume for the growth of crystals including halide perovskites via the inverse-temperature method^{14, 15}, temperature-cooling method¹⁶, antisolvent evaporation¹⁷ and extraction of solvent¹⁸, when the change rates of the system volume and the solubility are known.

For the cubic structure of crystals such as halide perovskites, we consider the growth of a cubic crystal in the following analysis.

Temporal evolution of a cubic crystal

For a cubic crystal of a in width, the volume and surface area of the crystal are a^3 and $6a^2$, respectively. This gives $V_c/S = a/6$. Equation (2) is simplified as

$$C_0(V_0 - a_0^3) = C(V - a^3) + \frac{a^3 - a_0^3}{\Omega} \quad (11)$$

Three different cases are discussed below. Analytical formulation of the temporal evolution of the crystal width is derived only for Case 1 - the crystal growth in a liquid system of constant volume at a constant temperature. The other two cases need the information of the evaporation rate or the extraction rate of solvent for Case 2 and the change rate of temperature and the temperature dependence of the solubility for Case 3. Numerical calculation is needed to find the temporal evolution of the crystal width.

Case 1: Isothermal growth in a liquid system of constant volume

For isothermal growth of a cubic crystal in a liquid system of constant volume, there are no evaporation and extraction of solvent during the crystal growth. We have $dC_s/dt = 0$ and $dV/dt = 0$ ($V = V_0$). The second equation in Eq. (9) gives

$$C = \frac{D + k\delta}{2kD\Omega} \frac{da}{dt} + C_s \quad (12)$$

Substituting Eq. (12) in Eq. (11) with $V = V_0$ yields

$$C_0(V_0 - a_0^3) = \left(\frac{D + k\delta}{2kD\Omega} \frac{da}{dt} + C_s \right) (V_0 - a^3) + \frac{a^3 - a_0^3}{\Omega} \quad (13)$$

which can be re-written as

$$\frac{D + k\delta}{2kD\Omega} \frac{da}{dt} = \left(\frac{1}{\Omega} - C_s \right) - \left(\frac{1}{\Omega} - C_0 \right) \frac{V_0 - a_0^3}{V_0 - a^3} \quad (14)$$

Note that Eq. (14) can be obtained from Eq. (10). Using the initial condition of $a|_{t=0} = a_0$, we obtain the solution of Eq. (14) as

$$\frac{2kD}{D+k\delta}(1-\Omega C_s)t = a - a_0 + \frac{(1-\Omega C_0)(V_0 - a_0^3)}{\sqrt{3}(1-\Omega C_s)} \cdot V^{1/3}. \quad (15)$$

$$\left(\tan^{-1} \frac{1+2aV^{1/3}}{\sqrt{3}} - \tan^{-1} \frac{1+2a_0V^{1/3}}{\sqrt{3}} + \frac{\sqrt{3}}{6} \ln \frac{(V - a^3)}{(V - a_0^3)} \cdot \frac{(V^3 - a_0^3)}{(V^3 - a)^3} \right)$$

Here, the parameter $V^{1/3}$ is calculated as

$$V^{1/3} = V_0 - \frac{(1-\Omega C_0)(V_0 - a_0^3)}{1-\Omega C_s} \quad (16)$$

It needs to be pointed out that the volume of the liquid solution at the outset of growth is likely different from the combination of the volume of the liquid solution and the volumetric change of the cubic crystal at time t , because the space occupied by a monomer in the liquid solution is not simply equal to that in the crystal due to the difference in the interaction with adjacent materials²⁵. Therefore, the system is generally unable to maintain a constant volume. The contribution of the volumetric change of the cubic crystal to the change of the system volume can be approximated to be a linear function of the volumetric change of the cubic crystal to a first order of approximation, which can be incorporated in Eq. (10). However, the contribution of the volumetric change of the cubic crystal to the change of the system volume is generally negligible in most cases and it is reasonable to assume that the system volume maintains unchanged under isolated condition.

Consider the growth of a CsPbBr₃ crystal of cubic phase in water. The molar mass and density of CsPbBr₃ crystal of cubic phase are 579.8175 g/mol²⁶ and 4.42 g/cm³²⁷. The lattice constant of CsPbBr₃ crystal of cubic phase is 0.6017 nm²⁷, and the solubility of CsPbBr₃ crystal of cubic phase in water is 0.047 g/mL at 23 °C²⁸. Using the molar mass and density of CsPbBr₃ crystal of cubic phase, we obtain the molar volume of CsPbBr₃ crystal of cubic phase as 131.18 mL/mol and the solubility of CsPbBr₃ of cubic phase in water as 8.11×10⁻⁵ mol/mL.

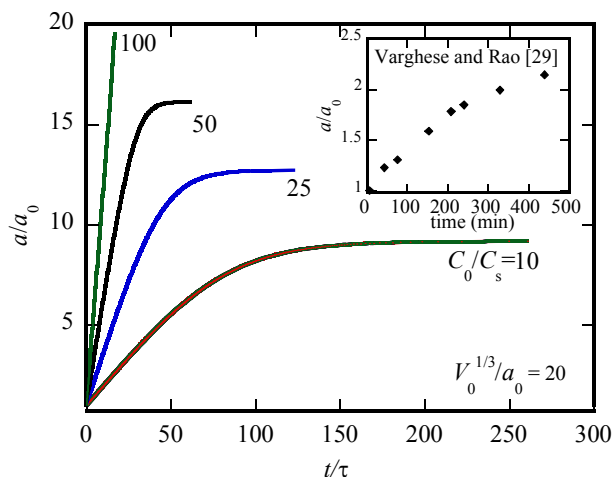


Figure 2. Temporal evolution of the sizes of cubic crystals of cubic phase for different degrees of supersaturation ($V_0^{1/3}/a_0 = 20$). The embedded figure shows the experimental results for the growth of Pt nanocrystals from the work of Varghese and Rao ²⁹.

Define $\tau = (D + k\delta)a_0/2kD(1-\Omega C_s)$. Figure 2 depicts temporal evolution of the sizes of CsPbBr₃ crystals of cubic phase for $V_0^{1/3}/a_0 = 20$ and different degrees of supersaturation. It is interesting to note that there are three stages for the growth of the cubic crystals – the sizes of the cubic crystals increase linearly with the growth time in the first stage, nonlinearly with the growth time in the second stage and reach plateau in the third stage. The linear stage is consistent with the observations by Varghese and Rao ²⁹ for the growth of Pt nanocrystals and Jung et al. ³⁰ for the growth of gold spiky nanoparticles in a liquid cell and the analysis by Yang ²³ for diffusion-limited growth of a nanoparticle in a finite space. The second stage is associated with the competition between the diffusion-limited growth and the reaction-limited growth due to the decrease in the degree of supersaturation. The third stage corresponds to the depletion of the monomers in the solution, which hinders the further growth of the cubic crystals.

For the purpose of qualitative comparison, the experimental results for the growth of Pt nanocrystals in a liquid solution with chloroplatinic acid and sodium citrate from the work of Varghese and Rao ²⁹ is included in Fig. 2. It is evident that there are two stages for the growth of Pt nanocrystals with an initially linear stage followed by a nonlinear stage, qualitatively in accord with the trend revealed by the numerical results in Fig. 2. The similar trend suggests that

one can use the model to determine the diffusivity and the reaction rate for the growth under isothermal and isochoric conditions.

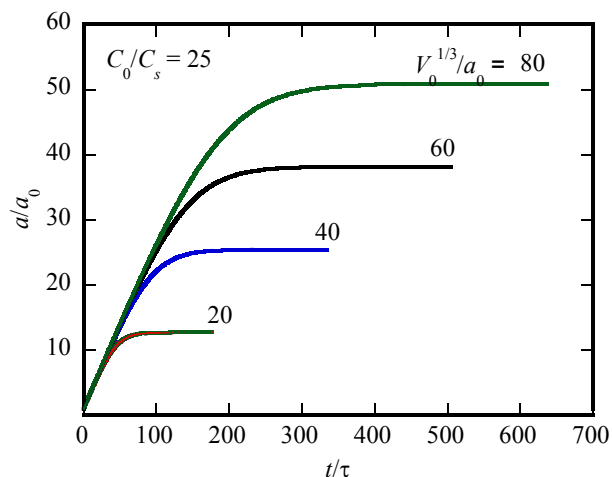


Figure 3. Temporal evolution of the sizes of cubic crystals for $C_0/C_s = 25$ and different ratios of $V_0^{1/3}/a_0$.

Figure 3 shows the temporal evolution of the sizes of cubic crystals for $C_0/C_s = 25$ and different ratios of $V_0^{1/3}/a_0$. It is interesting to note that there exists an overlap region for the linear growth stage for the growth of the cubic crystals in the systems with $C_0/C_s = 25$ for different ratios of $V_0^{1/3}/a_0$. Such a result suggests that the growth rate of $d(a/a_0)/d(t/\tau)$ in the linear growth stage is only dependent of the degree of supersaturation and independent of the system size. Note that both the period for the linear growth stage and the crystal size in the third stage increase with the increase of the ratio of $V_0^{1/3}/a_0$, revealing the effects of the amount of monomers on the growth and size of cubic crystals.

Figure 4 shows the variation of the growth rate of cubic crystals in the linear growth stage with the initial concentration of monomers ($C_0 = nC_s$ with n being unitless) for $V_0^{1/3}/a_0 = 20$. The growth rate increases linearly with the increase of the initial concentration of monomers (nC_s), indicating the importance of the degree of supersaturation in controlling the initial growth of the cubic crystals.

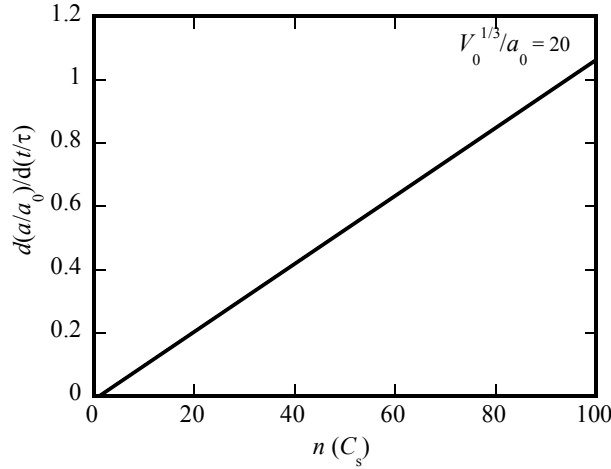


Figure 4. Dependence of the growth rate of cubic crystals in the linear growth stage on the initial concentration of monomers ($C_0 = nC_s$ with n being unitless) for $V_0^{1/3} / a_0 = 20$.

Case 2: Isothermal growth in a liquid system with evaporation and/or extraction of solvent

For isothermal growth of a cubic crystal in a liquid system with evaporation and/or extraction of solvent^{17, 18}, we have $dC_s/dt = 0$. Let $\alpha(t)$ be the decreasing rate of the volume of the liquid system, which is associated with the rate of the evaporation and/or extraction of solvent. The volume of the system at the growth time t becomes

$$V = V_0 - \int_0^t \alpha(t) dt \quad (17)$$

Substituting Eq. (17) in Eq. (11), we have

$$C_0 (V_0 - a_0^3) = \left(\frac{D + k\delta}{2kD\Omega} \frac{da}{dt} + C_s \right) \left(V_0 - \int_0^t \alpha(t) dt - a^3 \right) + \frac{a^3 - a_0^3}{\Omega} \quad (18)$$

It is evident that the rate of the evaporation and/or extraction of solvent plays an important role in the temporal evolution of the crystal in a liquid solution in a finite space. Equation (18) is a nonlinear differential equation, which can be only solved numerically if $\alpha(t)$ is known.

From Eq. (18), the growth rate of the size of the cubic crystal can be expressed as

$$\frac{da}{dt} = \frac{2kD\Omega}{D + k\delta} \left\{ \left[C_0 (V_0 - a_0^3) - \frac{a^3 - a_0^3}{\Omega} \right] \left(V_0 - \int_0^t \alpha(t) dt - a^3 \right)^{-1} - C_s \right\} \quad (19)$$

It is evident that the larger the rate of the evaporation and/or extraction of solvent, the larger is the growth rate of the size of the cubic crystal for the same size of the cubic crystal. That is to say, increasing the rate of the evaporation and/or extraction of solvent leads to fast growth of the cubic crystal, which is due to the increase of the supersaturation degree. It should be noted that the increase of the supersaturation degree also can increase the probability to form more nuclei during the growth, which can reduce the concentration of monomers and lead to the formation and growth of multiple crystals. An optimized rate of the evaporation and/or extraction of solvent needs to be determined to limit the formation of more nuclei during the growth in order to grow crystals of large sizes.

Under a constant rate of the evaporation and/or extraction of solvent, one can numerically integrate Eq. (19). The numerical results can then be compared with experimental results, and the diffusivity and the reaction rate can be numerically determined for the growth of the cubic crystals.

Case 3: Isochoric growth in a liquid system with the change in temperature

For isochoric growth of a cubic crystal in a liquid system with the change in temperature¹⁴⁻¹⁶, there is $dV/dt = 0$. According to the theory of thermodynamics, the solubility of monomers in a liquid solution is dependent on temperature. Assume that temperature is uniformly distributed in the liquid solution during the temperature change and the thermal-induced convection is negligible.

Using Eq. (10), we have

$$(V_0 - a^3) \left[\frac{D + k\delta}{2kD\Omega} \frac{d^2 a}{dt^2} + \frac{dC_s}{dt} \right] + \frac{3a^2}{\Omega} \left[1 - \frac{D + k\delta}{2kD} \frac{da}{dt} - \Omega C_s \right] \frac{da}{dt} = 0 \quad (20)$$

For C_s being a sole function of temperature T , we have

$$\frac{dC_s}{dt} = \frac{dC_s}{dT} \cdot \frac{dT}{dt} \quad (21)$$

Substituting Eq. (21) in Eq. (20) yields

$$(V_0 - a^3) \left[\frac{D + k\delta}{2kD\Omega} \frac{d^2 a}{dt^2} + \frac{dC_s}{dT} \cdot \frac{dT}{dt} \right] + \frac{3a^2}{\Omega} \left[1 - \frac{D + k\delta}{2kD} \frac{da}{dt} - \Omega C_s \right] \frac{da}{dt} = 0 \quad (22)$$

which is the differential equation for the analysis of the temporal evolution of the cubic crystal during the isochoric growth via the inverse-temperature method^{14, 15} or the temperature-cooling method¹⁶. Note that dC_s/dT in Eq. (22) is a function of time, which depends on the change rate of temperature.

It should be noted that both the diffusivity, D , and reaction rate, k , are dependent on temperature as

$$D = D_0 e^{-Q_d/R_g T} \quad \text{and} \quad k = k_0 e^{-Q_r/R_g T} \quad (23)$$

which suggest that the influx to the cubic crystal is dependent on temperature. Here, D_0 and k_0 are two pre-factors, Q_d and Q_r represent the activation energies for the diffusion and surface reaction, respectively, and R_g is the gas constant. Substituting Eq. (23) in Eq. (22) yields

$$\begin{aligned} (V_0 - a^3) \left[\frac{1}{2\Omega} \left(\frac{e^{Q_r/R_g T}}{k_0} + \frac{\delta e^{Q_d/R_g T}}{D_0} \right) \frac{d^2 a}{dt^2} + \frac{dC_s}{dT} \cdot \frac{dT}{dt} \right] \\ + \frac{3a^2}{\Omega} \left[1 - \frac{1}{2} \left(\frac{e^{Q_r/R_g T}}{k_0} + \frac{\delta e^{Q_d/R_g T}}{D_0} \right) \frac{da}{dt} - \Omega C_s \right] \frac{da}{dt} = 0 \end{aligned} \quad (24)$$

The nonlinearity of Eq. (24) indicates that numerical method is needed to find the temporal evolution of the crystal size if the temporal variation of temperature is known.

Comparing Eq. (24) with Eqs. (18) and (14), we note that the growth behavior for the isochoric growth of a cubic crystal with the change in temperature follows a second-order nonlinear differential equation instead of a first order nonlinear differential equation for isothermal growth. Such a difference suggests that the isochoric growth of a cubic crystal with the change in temperature is much more complex than the isothermal growth of the cubic crystal and it is much more difficult to control the growth of crystals. It is suggested that a combination of isothermal growth with multi-step changes of the growth temperature is used in the growth of crystals instead of the continuous change in the growth temperature used in the inverse-temperature method for the growth of crystals.

Discussion

The above analysis has been limited to the growth of a single crystal in a liquid system. Generally, there are significant numbers of crystals present in a liquid system during the crystal growth, i.e. the growth is a multi-crystal problem. For simultaneous growth of multiple crystals present in a liquid system of constant volume, Eq. (2) is modified as

$$C_0 \left(V_0 - \frac{1}{\rho} \sum_{i=1}^n M_{i0} \right) = C \left(V_0 - \frac{1}{\rho} \sum_{i=1}^n M_i \right) + \frac{1}{\rho \Omega} \left(\sum_{i=1}^n (M_i - M_{i0}) \right) \quad (25)$$

with M_{i0} as the initial mass of the i -th crystal and M_i as the mass of the i -th crystal at the growth time t . Taking derivative with respect to the growth time t for both sides of Eq. (25), we have

$$\left(V_0 - \frac{1}{\rho} \sum_{i=1}^n M_i \right) \frac{dC}{dt} + \frac{1 - \Omega C}{\rho \Omega} \sum_{i=1}^n \frac{dM_i}{dt} = 0 \quad (26)$$

According to the photoluminescence (PL) spectrum of semiconductor nanocrystals³¹, the PL intensity as a function of the emission wavelength approximately follows a Gaussian distribution function. It is known that the PL intensity is proportional to the concentration of nanocrystals and the reciprocal of the emission wavelength is a linear function of the reciprocal of the square of nanocrystal size. Therefore, we can assume that the size distribution of cubic crystals can be approximately described by a Gaussian distribution as

$$f(x) = \frac{1}{\sqrt{2\pi\sigma^2}} e^{-\frac{(x-x_0)^2}{2\sigma^2}} \quad (27)$$

with x_0 as the mean size of the cubic crystals and σ as the standard deviation. Therefore, there are

$$\begin{aligned} \sum_{i=1}^n M_i &= \rho \sum_{i=1}^n V_i = \rho \sum_{i=1}^n x_i^3 \approx \frac{\rho}{\sqrt{2\pi\sigma^2}} \int_0^\infty x^3 e^{-\frac{(x-x_0)^2}{2\sigma^2}} dx \\ &\approx \frac{\rho}{\sqrt{2\pi\sigma^2}} \int_{-\infty}^\infty x^3 e^{-\frac{(x-x_0)^2}{2\sigma^2}} dx = \frac{\rho}{\sqrt{2\pi\sigma^2}} (x_0^3 + 3\sigma^2 x_0) \end{aligned} \quad (28)$$

Substituting Eq. (28) in Eq. (26) yields

$$\left[V_0 - \frac{1}{\sqrt{2\pi\sigma^2}} (x_0^3 + 3\sigma^2 x_0) \right] \frac{dC}{dt} + \frac{3}{\sqrt{2\pi\sigma^2}} \frac{1 - C\Omega}{\Omega} \left[(x_0^2 + \sigma^2) \frac{dx_0}{dt} + 2\sigma x_0 \frac{d\sigma}{dt} \right] = 0 \quad (29)$$

from which we note that the monomer concentration in a liquid solution during the growth of multiple crystals is dependent on the change rates of the average size and the standard deviation of the crystal sizes. The change rate of the average size of the multiple crystals, which is likely associated with the Ostwald ripening process, is dependent on the change rates of the standard deviation and the monomer concentration.

Generally, it is very difficult to measure the diffusivity and the reaction rate involving in the growth of crystals in liquid solution. The model presented in this work establish the correlation between the growth rate of the size of cubic crystals in a liquid solution in a finite space and the growth conditions, which can be used to evaluate the temporal evolution of the crystal size. Comparing the numerical results from the modeling analysis with the experimental results for the crystal growth under given conditions, one can determine the dominant rate process controlling the growth of crystals and the important rate parameters of diffusivity and reaction rate.

Conclusion

Understanding the growth behavior of nanoparticles and nanocrystals in liquid solutions is of practical importance in controlling the sizes of nanoparticles and nanocrystals for engineering applications. Following the approach given by Sung et al.²⁰, we have developed a general formulation for the growth of a crystal/particle in a liquid solution. This formulation takes account of the combinational effect of the diffusion-limited growth and the reaction-limited growth and incorporates the effects of the volumetric change of the liquid system and the change of the solubility of the crystal/particle in the liquid solution.

We have considered three special growth scenarios for the growth of a cubic crystal – Case 1 without the change in the volume of the liquid system under isothermal condition, Case 2 with the change in the volume of the liquid system under isothermal condition, and Case 3 without the change in the volume of the liquid system and with temperature change. Closed-form solution for the temporal evolution of the size of a cubic crystal is obtained for Case I. The numerical results reveal that there are three growth stages – linear growth, nonlinear growth and plateau for the growth under the Case 1 conditions. The degree of supersaturation controlling the initial growth and the final size of the cubic crystal.

The growth behavior for the isochoric growth of a cubic crystal with the change in temperature is much more complex than the isothermal growth of the cubic crystal, and it is much more difficult to control the growth of crystals. A combination of isothermal growth with multi-step changes of the growth temperature is preferred in the growth of crystals instead of the continuous change in the growth temperature used in the inverse-temperature method for the growth of crystals.

For the growth of multiple crystals of different sizes in a liquid system without the changes in the volume of the liquid system and the solubility of the crystals/particles in the liquid solution, we have developed a mathematical formulation of the change of the monomer concentration under the assumption that the size distribution of the multiple crystals follows a Gaussian distribution function. The formulation reveals that the change rate of the average size of the multiple crystals, which is likely associated with the Ostwald ripening process, is dependent on the change rates of the standard deviation and the monomer concentration..

Acknowledgement

FY is grateful for the support by the NSF through the grant CMMI-1854554, monitored by Drs. Khershed Cooper and Thomas Francis Kuech, and CBET- 2018411 monitored by Dr. Nora F Savage.

References:

1. Eperon, G. E.; Burlakov, V. M.; Docampo, P.; Goriely, A.; Snaith, H. J., Morphological control for high performance, solution-processed planar heterojunction perovskite solar cells. *Advanced Functional Materials* **2014**, *24*, 151-157.
2. Zhang, F.; Lu, H.; Tong, J.; Berry, J. J.; Beard, M. C.; Zhu, K., Advances in two-dimensional organic–inorganic hybrid perovskites. *Energy & Environmental Science* **2020**, *13*, 1154-1186.
3. Jeong, M.; Choi, I. W.; Go, E. M.; Cho, Y.; Kim, M.; Lee, B.; Jeong, S.; Jo, Y.; Choi, H. W.; Lee, J., Stable perovskite solar cells with efficiency exceeding 24.8% and 0.3-V voltage loss. *Science* **2020**, *369*, 1615-1620.
4. Cao, Y.; Wang, N.; Tian, H.; Guo, J.; Wei, Y.; Chen, H.; Miao, Y.; Zou, W.; Pan, K.; He, Y., Perovskite light-emitting diodes based on spontaneously formed submicrometre-scale structures. *Nature* **2018**, *562*, 249-253.
5. Lin, K.; Xing, J.; Quan, L. N.; de Arquer, F. P. G.; Gong, X.; Lu, J.; Xie, L.; Zhao, W.; Zhang, D.; Yan, C., Perovskite light-emitting diodes with external quantum efficiency exceeding 20 per cent. *Nature* **2018**, *562*, 245-248.
6. Wei, W.; Zhang, Y.; Xu, Q.; Wei, H.; Fang, Y.; Wang, Q.; Deng, Y.; Li, T.; Gruverman, A.; Cao, L., Monolithic integration of hybrid perovskite single crystals with heterogenous substrate for highly sensitive X-ray imaging. *Nature Photonics* **2017**, *11*, 315-321.
7. Xing, G.; Mathews, N.; Lim, S. S.; Yantara, N.; Liu, X.; Sabba, D.; Grätzel, M.; Mhaisalkar, S.; Sum, T. C., Low-temperature solution-processed wavelength-tunable perovskites for lasing. *Nature Materials* **2014**, *13*, 476-480.
8. de Quilettes, D. W.; Vorpahl, S. M.; Stranks, S. D.; Nagaoka, H.; Eperon, G. E.; Ziffer, M. E.; Snaith, H. J.; Ginger, D. S., Impact of microstructure on local carrier lifetime in perovskite solar cells. *Science* **2015**, *348*, 683-686.
9. Jeon, N. J.; Noh, J. H.; Yang, W. S.; Kim, Y. C.; Ryu, S.; Seo, J.; Seok, S. I., Compositional engineering of perovskite materials for high-performance solar cells. *Nature* **2015**, *517*, 476-480.

10. Ye, F.; Chen, H.; Xie, F.; Tang, W.; Yin, M.; He, J.; Bi, E.; Wang, Y.; Yang, X.; Han, L., Soft-cover deposition of scaling-up uniform perovskite thin films for high cost-performance solar cells. *Energy & Environmental Science* **2016**, *9*, 2295-2301.
11. Brenner, T. M.; Egger, D. A.; Kronik, L.; Hodes, G.; Cahen, D., Hybrid organic-inorganic perovskites: low-cost semiconductors with intriguing charge-transport properties. *Nature Reviews Materials* **2016**, *1*, 1-16.
12. Al-Ashouri, A.; Köhnen, E.; Li, B.; Magomedov, A.; Hempel, H.; Caprioglio, P.; Márquez, J. A.; Vilches, A. B. M.; Kasparavicius, E.; Smith, J. A., Monolithic perovskite/silicon tandem solar cell with > 29% efficiency by enhanced hole extraction. *Science* **2020**, *370*, 1300-1309.
13. Xu, W.; Hu, Q.; Bai, S.; Bao, C.; Miao, Y.; Yuan, Z.; Borzda, T.; Barker, A. J.; Tyukalova, E.; Hu, Z., Rational molecular passivation for high-performance perovskite light-emitting diodes. *Nature Photonics* **2019**, *13*, 418-424.
14. Saidaminov, M. I.; Abdelhady, A. L.; Murali, B.; Alarousu, E.; Burlakov, V. M.; Peng, W.; Dursun, I.; Wang, L.; He, Y.; Maculan, G., High-quality bulk hybrid perovskite single crystals within minutes by inverse temperature crystallization. *Nature Communications* **2015**, *6*, 1-6.
15. Liu, Y.; Yang, Z.; Cui, D.; Ren, X.; Sun, J.; Liu, X.; Zhang, J.; Wei, Q.; Fan, H.; Yu, F., Two-inch-sized perovskite $\text{CH}_3\text{NH}_3\text{PbX}_3$ (X= Cl, Br, I) crystals: growth and characterization. *Advanced Materials* **2015**, *27*, 5176-5183.
16. Dang, Y.; Liu, Y.; Sun, Y.; Yuan, D.; Liu, X.; Lu, W.; Liu, G.; Xia, H.; Tao, X., Bulk crystal growth of hybrid perovskite material $\text{CH}_3\text{NH}_3\text{PbI}_3$. *CrystEngComm* **2015**, *17*, 665-670.
17. Shi, D.; Adinolfi, V.; Comin, R.; Yuan, M.; Alarousu, E.; Buin, A.; Chen, Y.; Hoogland, S.; Rothenberger, A.; Katsiev, K., Low trap-state density and long carrier diffusion in organolead trihalide perovskite single crystals. *Science* **2015**, *347*, 519-522.
18. Yao, F.; Peng, J.; Li, R.; Li, W.; Gui, P.; Li, B.; Liu, C.; Tao, C.; Lin, Q.; Fang, G., Room-temperature liquid diffused separation induced crystallization for high-quality perovskite single crystals. *Nature Communications* **2020**, *11*, 1-9.

19. Zhang, F.; Zhong, H.; Chen, C.; Wu, X.-g.; Hu, X.; Huang, H.; Han, J.; Zou, B.; Dong, Y., Brightly luminescent and color-tunable colloidal $\text{CH}_3\text{NH}_3\text{PbX}_3$ (X= Br, I, Cl) quantum dots: potential alternatives for display technology. *ACS Nano* **2015**, *9*, 4533-4542.
20. Sung, M.-H.; Kim, J.-S.; Kim, W.-S.; Hirasawa, I.; Kim, W.-S., Modification of crystal growth mechanism of yttrium oxalate in metastable solution. *Journal of Crystal Growth* **2002**, *235*, 529-540.
21. Viswanatha, R.; Sarma, D. D., Growth of nanocrystals in solution. *Nanomaterials Chemistry: Recent Developments And New Directions*, edited by C. N. R. Rao, Achim Müller, Anthony K. Cheetham, Wiley-VCH Verlag GmbH & Co, Darmstadt **2007**, 139-170.
22. Myers, T.; Fanelli, C., On the incorrect use and interpretation of the model for colloidal, spherical crystal growth. *Journal of Colloid and Interface Science* **2019**, *536*, 98-104.
23. Yang, F., Diffusion-limited growth of a spherical nanocrystal in a finite space. *Langmuir* **2021**, *37*, 3912-3921.
24. Liu, Y.; Zhang, Y.; Yang, Z.; Feng, J.; Xu, Z.; Li, Q.; Hu, M.; Ye, H.; Zhang, X.; Liu, M., Low-temperature-gradient crystallization for multi-inch high-quality perovskite single crystals for record performance photodetectors. *Materials Today* **2019**, *22*, 67-75.
25. Yang, F. Q., Nucleation in a liquid droplet. *Phys Chem Chem Phys* **2020**, *22*, 9990-9997.
26. <https://www.webqc.org/molecular-weight-of-CsPbBr3.html>.
27. <https://materialsproject.org/materials/mp-600089/>.
28. Peng, J.; Xia, C. Q.; Xu, Y.; Li, R.; Cui, L.; Clegg, J. K.; Herz, L. M.; Johnston, M. B.; Lin, Q., Crystallization of CsPbBr_3 single crystals in water for X-ray detection. *Nature Communications* **2021**, *12*, 1-10.
29. Varghese, N.; Rao, C., Growth kinetics of platinum nanocrystals prepared by two different methods: Role of the surface. *Journal of Colloid and Interface Science* **2012**, *365*, 117-121.
30. Jung, W.-G.; Park, J. H.; Jo, Y.-R.; Kim, B.-J., Growth kinetics of individual Au spiky nanoparticles using liquid-cell transmission electron microscopy. *Journal of the American Chemical Society* **2019**, *141*, 12601-12609.
31. Zhang, C.; Luan, W.; Huang, Y.; Yang, F., Growth of perovskite nanocrystals in poly-tetra fluoroethylene based microsystem: on-line and off-line measurements. *Nanotechnology* **2019**, *30*, 145602.